ADVANCED FUNCTIONAL MATERIALS
www.afm-journal.de

Exceptional Oxygen Sensing Properties of New Blue Light-Excitable Highly Luminescent Europium(III) and Gadolinium(III) Complexes

Sergey M. Borisov, Roland Fischer, Robert Saf, and Ingo Klimant*

New europium(III) and gadolinium(III) complexes bearing 8-hydroxyphenalenone antenna combine efficient absorption in the blue part of the spectrum and strong emission in polymers at room temperature. The Eu(III) complexes show characteristic red luminescence whereas the Gd(III) dyes are strongly phosphorescent. The luminescence quantum yields are about 20% for the Eu(III) complexes and 50% for the Gd(III) dyes. In contrast to most state-of-the-art Eu(III) complexes the new dyes are quenched very efficiently by molecular oxygen. The luminescence decay times of the Gd(III) complexes exceed 1 ms which ensures exceptional sensitivity even in polymers of moderate oxygen permeability. These sensors are particularly suitable for trace oxygen sensing and may be good substitutes for Pd(II) porphyrins. The photophysical and sensing properties can be tuned by varying the nature of the fourth ligand. The narrow-band emission of the Eu(III) allows efficient elimination of the background light and autofluorescence and is also very attractive for use e.g., in multi-analyte sensors. The highly photostable indicators incorporated in nanoparticles are promising for imaging applications. Due to the straightforward preparation and low cost of starting materials the new dyes represent a promising alternative to the state-of-the-art oxygen indicators particularly for such applications as, e.g., food packaging.

1. Introduction

Monitoring of oxygen is of high importance in numerous fields of science and technology. Optical oxygen sensors proved to be reliable analytical tools and represent a promising alternative to the Clark electrode. The materials used in optical oxygen sensors are quite established.[1–4] Most oxygen sensors employ such widespread indicators as ruthenium(II) polypyridyl complexes,[5–7] platinum(II) and palladium(II) porphyrins[8–11] and their analogues.[12–14] Other luminescent indicators are less popular which is explained by their inferior photophysical properties (low absorption coefficients and luminescence quantum yields, short luminescence decay times, poor photostability etc.)[3] or by complicated multi-step synthesis. Such indicators as cyclometalated iridium(III) and platinum(II) complexes,[15–17] osmium(II),[18] rhenium(I)[19] and copper(I)[20,21] complexes should also be mentioned. Europium(III) complexes represent a particularly interesting group of luminescent compounds which are distinguished by their very large Stokes shifts, long luminescence decay times (hundreds of μs – few ms) and very narrow emission bands.[22] These complexes are widely applied as labels in various luminescence assays both as free dyes bearing a functional group for conjugation and in the form of dye-doped nanoparticles,[22,23] but application in optical sensors and analyte-sensitive probes is comparably rare.[24–27] For example, luminescent Eu(III) complexes were applied as optical temperature probes,[27–31] pH indicators,[32–36] fluoroionophores for bicarbonate,[37,38] citrate[39] and lactate[40] and as hydrogen peroxide[41] and nitrogen monooxide probes.[42] Several Eu(III) complexes were applied as luminescent oxygen indicators.[43–48] However, the sensitivity of these oxygen-sensing materials is rather low (quenching at 100% O_2 I_0/I not exceeding 3-4) for them to be suitable for measurements in physiologically relevant conditions with good resolution. Moreover, UV light was required for the excitation of all the indicators which is not attractive for many reasons. The number of Eu(III) complexes excitable in the visible part of electromagnetic spectrum is very limited. The drawbacks include low luminescence brightness,[37,41,49] poor chemical stability,[50] extremely laborious multi-step synthesis[51] or rather poor photostability.[30,52]

The sensing properties of Gd(III) complexes remain mostly unexplored. Despite the fact that these complexes are widely

Dr. S. M. Borisov, Prof. I. Klimant
Institute of Analytical Chemistry
and Food Chemistry
Graz University of Technology
NAWI Graz
Stremayrgasse 9 8010, Graz, Austria
E-mail: sergey.borisov@tugraz.at
Prof. R. Fischer
Institute of Inorganic Chemistry
Graz University of Technology
NAWI Graz
Stremayrgasse 9 8010, Graz, Austria
Prof. R. Saf
Institute of Chemistry and Technology of Materials
Graz University of Technology
NAWI Graz
Stremayrgasse 9 8010, Graz, Austria

DOI: 10.1002/adfm.201401754

used for determination of the triplet state energy of the respective ligands at 77K there are very few reports on luminescence of the Gd(III) chelates at room temperature (RT). For example, Strasser and Vogler reported on luminescence of UV light-excitable chelates at RT[53]; we[54] and others[55] recently demonstrated that some Gd(III) chelates also possess viable luminescence at RT. Much lower cost of europium and gadolinium compared to the cost of platinum group metals can make them attractive substitutes to the state-of-the-art indicators providing that the photophysical properties are more favorable and quenching by oxygen is efficient. Additionally, Gd(III) may be promising as materials for simultaneous oxygen and magnetic resonance imaging, which is by far the most important application of the non-emissive Gd(III) chelates.[56–58]

In this contribution we will present a series of new Eu(III) and Gd(III) complexes which combine efficient excitation in the blue part of the electromagnetic spectrum, strong emission and efficient quenching by molecular oxygen. It will be shown that 9-hydroxy-1*H*-phenalen-1-one, in contrast to an early report,[59] represents an efficient antenna for sensitizing luminescence of the lanthanides under visible light and thus represents an excellent choice for preparation of high-performance optical materials. We will demonstrate the application of the complexes in optical oxygen sensors and will highlight the advantages over the state-of-the-art indicators.

2. Experimental Section

2.1. Materials

Gadolinium(III) nitrate hexahydrate, 4,7-diphenyl-1,10-phenanthroline (= dpp), 10-(2-benzothiazolyl)-2,3,6,7-tetrahydro-1,1,7,7-tetramethyl-1H,5H,11H-(1)benzopyropyrano(6,7-8-I,j) quinolizin-11-one (coumarin C 545 T) and aqueous dispersion of polystyrene-block-vinylpyrrolidone (= PS-PVP) were obtained from Aldrich, europium(III) chloride hexahydrate was from ABCR, 1,10-phenanthroline monohydrate – from Merck, polystyrene (MW 250,000) – from Acros Organics. Polymethacrylonitrile (= PMAN, MW = 20,000) was acquired from Scientific Polymer Products Inc. (Ontario, NY, USA) and Eudragit Rl-100 from Evonic Industries (Essen, Germany). All the solvents were supplied by Carl Roth (Germany). Poly(ethylene terephthalate) (PET) support Melinex 505 was from Pütz (Taunusstein, Germany). Nitrogen (99.999% purity) was obtained from Linde Gas (Austria). Synthesis of the 9-hydroxy-1*H*-phenalen-1-one (= HPhN) is described elsewhere.[60] 1,1′-(9,9-dimethyl-9H-xanthene-4,5-diyl)bis-1,1-diphenyl-phosphine oxide (DDXPO) was prepared according to the literature procedure.[61]

2.2. Synthesis

Europium(III)/gadolinium(III) tris-[9-(hydroxy-kO)-1H-phenaleno-1-onato-kO] (Eu(HPhN)$_3$/Gd(HPhN)$_3$): First, europium(III) chloride hexahydrate (488 mg, 1.32 mmol) or gadolinium(III) nitrate hexahydrate (596 mg, 1.32 mmol), respectively, was dissolved in the mixture of water:ethanol mixture (1:4 v/v, 10 mL). This solution was added dropwise to the warm solution (70 °C) of HPhN (784 mg, 4 mmol) in 70 mL of ethanol containing 1 mL of 25% aqueous ammonium hydroxide. The heating was continued for 5-20 min. The progress of the reaction was controlled via UV–Vis spectroscopy and bathochromic shift of the absorption peaks in the visible part of the spectrum was observed. The obtained yellow precipitate was collected via centrifugation and was washed 3 times with water and once with water : methanol (1:1 v/v) mixture. The crude product was used without further purification. Yield: 760 mg (78 %) for Eu(HPhN)$_3$; MS (EI): m/z [M]$^+$ 736.0538 found, 736.0536 calc. Yield: 680 mg (69%) for Gd(HPhN)$_3$; MS (MALDI): m/z [MNa]$^+$ 766.05 found, 766.05 calc.

Europium(III)/gadolinium(III) tris-[9-(hydroxy-kO)-1H-phenaleno-1-onato-kO]-1,10 -phenanthroline (Eu(HPhN)$_3$phen/Gd(HPhN)$_3$phen): The solution of 1,10-phenanthroline monohydrate (19.8 mg , 0.1 mmol) in toluene (5 mL) was added dropwise to the hot dispersion of Eu(HPhN)$_3$ (73.7 mg, 0.1 mmol) or Gd(HPhN)$_3$ (74.3 mg, 0.1 mmol), respectively, in hot toluene (5 mL, 100 °C). The heating was continued for 1h, the resulted solution was rapidly cooled to room temperature and centrifuged to remove the remaining sediment. The X-ray quality crystals were grown by slow diffusion of hexane into the toluene solution at room temperature. Eu(HPhN)$_3$phen·1.25C$_7$H$_8$. Yield: 28 mg (31%). MS(MALDI) m/z [M – 1HPhN]$^+$ 723.0827 found, 723.0796 calc. Analysis for $C_{51}H_{29}N_2O_6Eu \cdot 1.25C_7H_8$: C 69.61, H 3.43, N 2.88 found, C 69.48, H 3.81, N 2.71 calc. Gd(HPhN)$_3$phen·0.75C$_7$H$_8$. Yield: 35 mg (38%). MS(MALDI) m/z [M – 1HPhN]$^+$ 728.0800 found, 728.0830 calc. Analysis for $C_{51}H_{29}N_2O_6Gd \cdot 0.75C_7H_8$: C 68.15, H 3.40, N 2.79 found, C 68.1, H 3.56, N 2.82 calc.

Europium(III)/gadolinium(III) tris-[9-(hydroxy-kO)-1H-phenaleno-1-onato-kO]-4,7-diphenyl-1,10-phenanthroline (Eu(HPhN)$_3$dpp/Gd(HPhN)$_3$dpp): The complexes were prepared analogously to Eu(HPhN)$_3$phen and Gd(HPhN)$_3$phen but 4,7-diphenyl-1,10-phenanthroline was used instead of 1,10-phenanthroline. Eu(HPhN)$_3$dpp·1C$_7$H$_8$. Yield: 38 mg (36%) of X-ray quality yellow crystals. MS(MALDI) m/z [M – 1HPhN]$^+$ 875.1367 found, 875.1425 calc. Analysis for $C_{63}H_{37}N_2O_6Eu \cdot 1C_7H_8$: C 72.20, H 3.76, N 2.35 found, C 72.33, H 3.9, N 2.41 calc. Gd(HPhN)$_3$dpp·0.75C$_7$H$_8$. Yield: 29 mg (27%) of X-ray quality yellow crystals. MS(MALDI) m/z [M – 1HPhN]$^+$ 880.1404 found, 880.1459 calc. Analysis for $C_{63}H_{37}N_2O_6Gd \cdot 0.75C_7H_8$: C 71.65, H 3.67, N 2.42 found, C 71.63, H 3.79, N 2.45 calc.

Europium(III)/gadolinium(III) tris-[9-(hydroxy-kO)-1H-phenaleno-1-onato-kO]-1,1′-(9,9-dimethyl-9H-xanthene-4,5-diyl)bis-1,1-diphenyl-phosphine oxide (Eu(HPhN)$_3$DDXPO/Gd(HPhN)$_3$DDXPO): The complexes were prepared analogously to Eu(HPhN)$_3$phen and Gd(HPhN)$_3$phen but DDXPO was used instead of 1,10-phenanthroline. After addition of DDXPO the hot toluene solution was filtered and the X-ray quality crystals were grown by slowly cooling the solution from 100 °C to room temperature (cooling rate 10 °C/h). Yield of Eu(HPhN)$_3$DDXPO: 54 mg (40%). MS(MALDI) m/z [M – 1HPhN]$^+$ 1153.195 found, 1153.194 calc. Analysis for $C_{78}H_{53}O_9P_2Eu$: C 68.94, H 3.70 found, C 69.49, H 3.96 calc. Yield of Gd(HPhN)$_3$DDXPO: 46 mg (34%). MS(MALDI) m/z [M – 1HPhN]$^+$ 1158.2017 found, 1158.1976 calc. Analysis for $C_{78}H_{53}O_9P_2Gd$: C 68.31, H 3.74, found, C 69.22, H 3.95. As indicated by the elemental analysis some impurity may be

present in the complex; however the composition of the complex were unambiguously confirmed by X-ray spectroscopy.

Preparation of the Oxygen Sensors: A lanthanide(III) complex (1.5 mg) and polystyrene (200 mg) were dissolved in toluene (1.8 g) and the resulted "cocktail" was knife-coated on the PET support to result in about 2.5 µm-thin films after evaporation of the solvent. The ratiometric sensors for RGB imaging were prepared analogously but the "cocktail" additionally contained 0.3 mg of coumarin C545T.

Preparation of the Nanoparticles: $Eu(HPhN)_3dpp$ was incorporated into PS-PVP nanoparticles according to the previously reported procedure.[62] The Rl-100 and PMAN beads were obtained via the precipitation procedure[63] from the polymer solutions in tetrahydrofuran:acetone (1:1 v/v). The concentration of the polymers in the solvent mixture was 0.2% wt. and fast addition of water was performed. All nanoparticles contained 1% wt. of the Eu(III) complex in respect to the polymer.

2.3. Measurements

Absorption spectra were measured on a Cary 50 UV–Vis spectrophotometer (Varian). Emission spectra were acquired on a Fluorolog 3 fluorescence spectrometer from Horiba (Japan) equipped with a NIR-sensitive photomultiplier R2658 from Hamamatsu (Japan). All the spectra were corrected for the sensitivity of the photomultiplier. The luminescence quantum yields in frozen glasses (77K, toluene:tetrahydrofuran 4:6 v/v) were determined relative to N,N´-bis-(2,6-diisopropylphenyl)-1,6,7,12-tetra-(4-phenoxy)perylene-3,4,9,10-tetracarboxylic acid diimide assuming $\Phi = 1$ in toluene/tetrahydrofuran glass at 77K ($\Phi = 0.96$ in chloroform at room temperature).[64] The absolute quantum yields for the sensors at room temperature were measured with an integrating sphere from Horiba. The sphere was thoroughly flushed with nitrogen prior to the measurement. Luminescence decay times were measured in a frequency domain with a two-phase lock-in amplifier (SR830, Stanford Research Inc., USA) equipped with a photomultiplier tube (H5701-02, Hamamatsu, Japan). The excitation was performed with the light of a 455-nm LED (Roithner Lasertechnik, Austria) filtered through a BG-12 filter from Schott (Germany). The emission was recorded using a combination of an OG-580 filter (Schott) and Calflex X filter from Linos. The modulation frequencies were 2.5, 2 kHz and 1.5 kHz for $Eu(HPhN)_3phen$, $Eu(HPhN)_3dpp$ and $Eu(HPhN)_3DDXPO$, respectively and 205, 180 and 145 Hz for the $Gd(HPhN)_3phen$, $Gd(HPhN)_3dpp$ and $Gd(HPhN)_3DDXPO$, respectively. The intensity-based quenching plots were obtained at the modulation frequencies of 165 Hz and 21 Hz for the Eu(III) and Gd(III) complexes, respectively. Gas calibration mixtures were obtained from nitrogen and compressed air using a gas mixing device from MKS (Andover, MA, USA). Temperature was controlled using a cryostat ThermoHaake DC50 (Thermo Fisher Scientific Inc). Luminescence decays at 77K were acquired on a Fluorolog 3 fluorescence spectrometer using a SpectraLED (λ_{exc} = 392 nm) and DeltaHub™ TCSPC unit from Horiba.

The size of the nanobeads was determined with a particle size analyzer Zetasizer Nano ZS from Malvern.

Photobleaching of the sensors was investigated using a high power blue LED array (Germany, www.led-tech.de) operated at 7.4 W input power; photon flux about 4000 $\mu mol \cdot s^{-1}m^{-2}$ of photons as estimated by a Li-250A Light meter from Li-COR. The absorption changes were monitored on a Cary 50 UV–Vis spectrophotometer.

RGB photographic imaging was performed with a Canon 5D digital camera equipped with a 24–105 mm f/4L IS objective from Canon. Excitation of the sensor foils was performed with a 366-nm line of a mercury lamp. The photographic images of the dispersions of the nanobeads were determined with the same equipment; however a blue 470 nm LED (Roithner) was used for the excitation. A plastic dark Amber filter from LEEfilters was used in front of the objective.

2.4. Crystal Structure Determination

Suitable crystals for X-ray structural analyses were selected and mounted on the tip of a glass fiber. Diffraction data were collected at 100 K on a Bruker D8 Kappa diffractometer equipped with a SMART APEX II CCD detector with Mo Kα (λ = 0.71073Å) radiation. Data were integrated with SAINT[65] and empirical methods as implemented in SADABS[66] were used to correct for absorption effects. Structures were solved with direct methods using SHELXS-97. SHELXL-97 was used for refinement against all data by full-matrix least-squares methods on F^2.[67] All non-hydrogen atoms were refined with anisotropic displacement parameters. Hydrogen atoms were refined isotropically on calculated positions using the riding model implemented in SHELXL-97. Tables containing crystallographic data and refinement parameters are given in the Supporting Information.

The crystal structures were visualized and the packing diagrams were generated using Mercury 3 visualization programme.[68] The files CCDC 971370-97135 contain the supplementary crystallographic data. These data can be obtained free of charge via www.ccdc.cam.ac.uk/conts/retrieving.html (or from the Cambridge Crystallographic Data Center, 12 Union Road, Cambridge CB2 1EZ, UK; fax +44 1223 336033; e-mail deposit@ ccdc.cam.ac.uk).

3. Results and Discussion

Synthesis and Structure of the Complexes: The europium(III) and gadolinium(III) complexes can be conveniently prepared in only two steps starting from readily available 8-hydroxyphenalenone (**Scheme 1**). This ligand can be synthesized in large quantities from cinnamoyl chloride and 2-methoxynaphthalene. The lanthanide salts used for complexes represent low cost materials which compare favorably with the price of platinum group metals used in most oxygen indicators. The intermediate complexes europium(III) and gadolinium(III) tris-[9-(hydroxy-k*O*)-1*H*-phenaleno-1-onato-k*O*] ($Eu(HPhN)_3$ and $Gd(HPhN)_3$, respectively) are poorly soluble in common solvents and their thorough purification was not performed. Instead, the crude materials were introduced in the second step in which a quaternary complex was formed (Scheme 1). The fourth ligand is

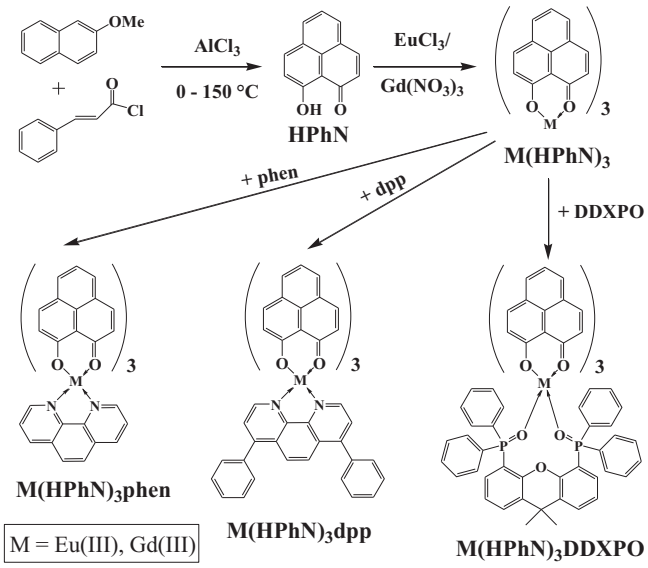

Scheme 1. Synthesis of the new Eu(III) complexes.

used to saturate the coordination sites of the metal in order to reduce the radiationless deactivation of the excited state and enhance the solubility. The solubility in common organic solvents indeed improves significantly. Due to the paramagnetic character of the central atom the nuclear magnetic resonance studies were not successful and the composition of the complexes was confirmed by mass spectrometry and elementary analysis. All the complexes were isolated as X-ray quality crystals. The X-ray spectroscopy unambiguously confirms the structure of the complexes and allows identification of the coordinated solvent molecules (**Figure 1**, Figure S1-S3).

The solid state structures of the complexes $M(HPhN)_3$phen, $M(HPhN)_3$dpp and $M(HPhN)_3$DDXPO (Eu, Gd) were studied by means of single crystal X-ray diffraction structure analyses. The molecular structures of the Eu(III) complexes are given in Figure 1, the respective Gd(III) derivatives are shown in the Supporting Information, Figure S1-S3. Selected bond distances and angles for all complexes are given in Table S1. Table S2 in the Supporting Information contains the crystallographic data for all compounds.

The crystals of $M(HPhN)_3$phen (M = Eu, Gd, both space group P2(1)/c) are isomorphous as are the two structures of $M(HPhN)_3$DDXPO (space group P-1). This is in contrast to the structures of the complexes based on the dpp ligand. In the latter case, the Eu(III) complex co-crystallizes in P-1 with two molecules of toluene per unit cell. The Gd-sample, however, also crystallizes in P-1, but in a unit cell about twice as large, where the asymmetric unit contains two molecules of the Gd(III)-complex and three molecules of co-crystallized toluene.

All compounds studied crystallographically exhibit eight-coordinate rare earth metal centers in the oxidation state +3. The average M-O distance between the rare earth metal ions and the oxygen atoms of the chelating HPhN ligands account to 2.364 Å for $Eu(HPhN)_3$phen and 2.362 Å $Eu(HPhN)_3$dpp, which is ca. 0.01 Å longer than in the respective Gd derivatives (2.356 Å in $Gd(HPhN)_3$phen and 2.350 Å in $Gd(HPhN)_3$dpp). These values agree very well with ionic radii of eight coordinate Eu(III) (r = 1.066 Å) and Gd(III) (r = 1.053 Å).[69] In all complexes studied, each of the coordinated HPhN ligands shows a pair of essentially identical C-O distances of ca. 1.27 Å, which is in between a C-O single bond (C(sp^2)-O 1.35 Å) and a double bond (C(sp^2)-O 1.21 Å).[70] In all complexes, the rare earth metal centers are located essentially in one plane with the ligand backbones of the HPhN, phen and dpp substituents.

Together with the almost identical M(III)-O^{HPhN} distances, this demonstrates the symmetrical bonding situation of the ligands and the metal center. Furthermore, the O-M(III)-O angles enclosed by the metal centers and the HPhN ligands show very little deviation from an average of ca 70°, which originates from the structural rigidity of the HPhN ligands. The coordination of the phenanthroline ligands phen and dpp in $M(HPhN)_3$phen and $M(HPhN)_3$dpp towards the central metal ions is again characterized by a strictly coplanar motif and slightly longer M(III)-N distances in the Eu(III) than the Gd(III) complexes. The even more constrained nature of the phenanthroline-based ligands is represented by acute N-M-N angles around 61°. In contrast, the O-M(III)-O angles in the phosphine oxide based complexes $Eu(HPhN)_3$DDXPO and $Gd(HPhN)_3$DDXPO are wider and account to ca. 74°. The higher flexibility of the ligand allows for a stronger interaction of the DDXPO ligand with the central metal ions which, as will be shown below, is also represented by bathochromic shifts in the UV–Vis spectra.

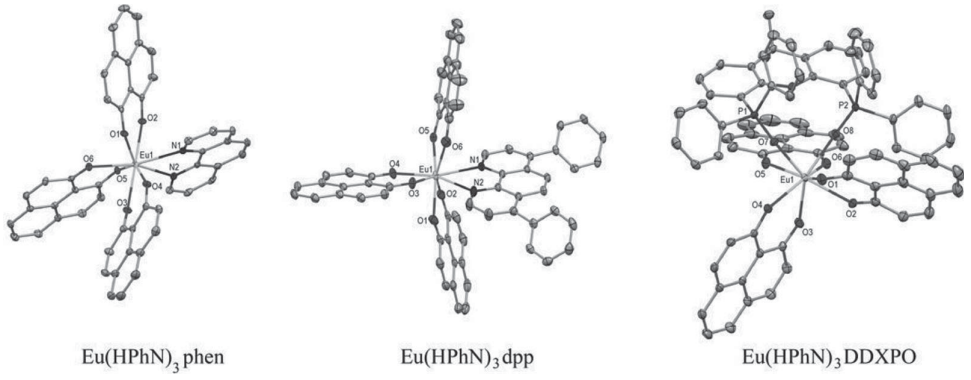

Figure 1. Thermal ellipsoid plots (50% probability) of the solid state molecular structures of the Eu(III) complexes. Hydrogen atoms have been omitted for clarity.

In comparison to the phen and dpp complexes, slightly elongated, yet also almost equidistant M-O bond lengths are observed in the phosphine oxide based complexes $M(HPhN)_3DDXPO$ (Eu, Gd). Overall, the structural properties correlate exceptionally well with results from optical spectroscopy, where almost identical spectra were found likewise for the pairs $Eu(HPhN)_3phen/Eu(HPhN)_3dpp$ and $Gd(HPhN)_3phen/Gd(HPhN)_3dpp$ and which are notably different from the respective DDXPO complexes.

Absorption Spectra: Similarly to the parent ligand all the complexes feature an intense absorption band in the UV region and two less intense bands in the blue part of the electromagnetic spectrum (**Figure 2**A). The position of the bands in the UV region is only minor affected by the complexation. On the other hand, a pronounced bathochromic shift of the absorption bands (21-23 nm or 1030-1130 cm^{-1}) located in the visible part of the spectrum is observed. The absorption spectra of $Eu(HPhN)_3phen$ and $Eu(HPhN)_3dpp$ are virtually identical (Figure 2A and Figure S4) but are slightly different from the spectra of $Eu(HPhN)_3DDXPO$. The same trend is observed for the respective Gd(III) complexes (Figure 2C). Notably, the absorption spectra of the Eu(III) complexes and the respective Gd(III) chelates are fully identical (Figure 2A and 2C, **Table 1**).

The longest absorption band in the complexes shows excellent overlap with the emission of a 465 nm blue LED which is one of the brightest LEDs available. This is particularly helpful for application of the dyes in compact sensing devices. The molar absorption coefficients of 25,000-30,000 $M^{-1}cm^{-1}$ (Table 1) are comparable to those of the most common oxygen indicators such as ruthenium(II) polypyridyl complexes and metalloporphyrins (for the Q bands in the visible part of the spectrum).[3]

Emission Spectra and Sensitization Mechanism: The europium(III) complexes in deoxygenated solutions show only very poor luminescence at room temperature (QYs about 1%). This is in good agreement with the results obtained by Van Deun et al.[59] (quantum yields of 0.5% for the tetrahydrofuran solution of $Eu(HPhN)_3$). However, the complexes possess very bright emission originating from the Eu(III) ion in frozen glasses at 77K (Figure 2B) and, as will be demonstrated below, in polymer matrices at room temperature. Enhancement of luminescence in frozen solutions at low temperatures and in highly viscous media is a rather common phenomenon. Poor luminescence in solutions at room temperature is often attributed to efficient radiativeless deactivation of the excited states involving e.g., solvent molecules and quenchers and is particularly pronounced for the long-lived triplet state. The emission of all the complexes is similar (Figure S5, Figure S6). Excitation with the UV light (350 nm, Figure S7) reveals very efficient energy transfer to the metal center since virtually no emission from the ligand is observed. The HPhN ligand is fluorescent at 77K but extremely week phosphorescence at about 540 nm is also observed (Figure 2B). Importantly, the excitation spectra of the complexes are virtually identical to the absorption spectra (Figure S8). The decay profiles in frozen solutions are adequately described by the mono-exponential model (Figure S9) and the calculated lifetimes are close to those obtained in the frequency domain measurements (Table 1).

The $^6P_{7/2}$ level of the Gd(III) (32105 cm^{-1})[71] is located well above the triplet states of the ligands so that the metal affects

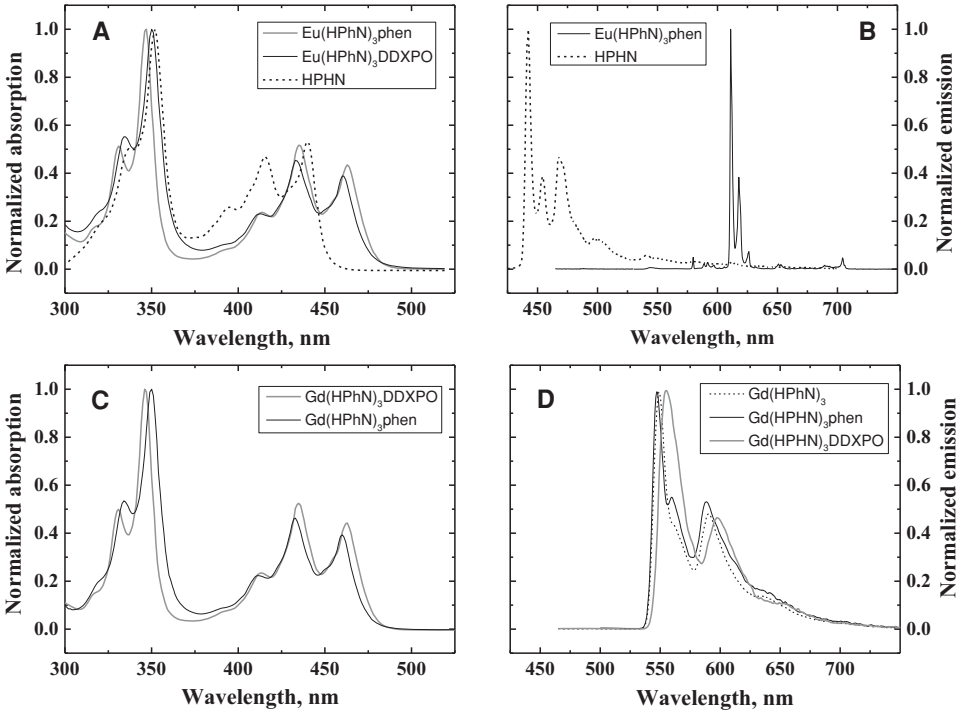

Figure 2. Spectral properties of the Eu(III) and Gd(III) complexes and the HPhN ligand. A and C: absorption spectra in toluene at room temperature. B and D: emission spectra in toluene:tetrahydrofuran (4:6 v/v) frozen glass (λ_{exc} = 460 for the Eu(III) and Gd(III) complexes and 400 nm for HPhN, respectively).

Table 1. Photophysical properties of the Eu(III) and Gd(III) complexes in solutions and in polystyrene.

Compound	λ_{max} abs (ε), nm ($M^{-1}\cdot cm^{-1}$)[a]	λ_{max} em,[b] nm	Φ[c]	τ,[b] μs	λ_{max} abs, nm[d]	λ_{max} em, nm[d]	Φ[d]	τ,[d] μs
HPhN	337 (10100); 352 (20000); 416 (9400); 440 (10700)	442	0.04	n.d.	n.d.	n.d.	n.d.	n.d.
$Eu(HPhN)_3$ phen	335 (39600); 350 (71500); 434 (32800); 461 (27500)[e]	611[f]	0.30	330[g]	335; 351; 434; 461	611[f]	0.18	94[g]
$Eu(HPhN)_3$ dpp	335 (45000); 350 (78100); 434 (34600); 461 (28800)[e]	611[f]	0.30	350[g]	335; 351; 434; 461	611[f]	0.18	110[g]
$Eu(HPhN)_3$ DDXPO	331 (35700); 347 (69000); 435 (35600); 463 (30000)	611[f]	0.70	400[g]	333; 348; 436; 463	611[f]	0.20	128[g]
$Gd(HPhN)_3$ phen	334 (32200); 350 (60000); 433 (27800); 460 (23600)[e]	547	0.34	6300[h] (52%) 1120 (48%)	336; 352; 435; 461	558	0.42	1280[g]
$Gd(HPhN)_3$ dpp	334 (39700); 350 (70300); 433 (32100); 460 (27300)[e]	547	0.77	3400[h] (38%) 840[h] (62%)	336; 351; 424; 461	558	0.56	1350[g]
)$Gd(HPhN)_3$ DDXPO	331 (32500); 346 (64800); 435 (33800); 463 (28400)	555	0.65	4100[h] (44%) 860 (56 %)	333; 348; 435; 462	563	0.53	2010[g]

[a]in toluene at room temperature; [b]in toluene at 77K; [c]in toluene/tetrahydrofuran frozen glass at 77K; [d]in polystyrene at 298K; [e]calculated for the dye containing no enclosed solvent molecules on basis of the elementary analysis data; [f]the peak with the highest intensity; [g]frequency domain measurement; [h]time domain measurement, Figure S11.

their photophysical properties solely by promoting inter-system crossing due to the heavy atom effect and paramagnetism. These properties of Gd(III) are helpful for determination of the triplet state energies at low temperature. All the Gd(III) complexes: $Gd(HPhN)_3$, $Gd(HPhN)_3$phen, $Gd(HPhN)_3$dpp and $Gd(HPhN)_3$DDXPO did not show any detectable fluorescence in frozen solutions at 77K but very strong phosphorescence (Figure 2D, Figure S10). The emission spectra of $Gd(HPhN)_3$phen and $Gd(HPhN)_3$dpp are very similar to the spectrum of $Gd(HPhN)_3$. The phosphorescence of $Gd(HPhN)_3$DDXPO is slightly shifted bathochromically (Figure 2D). The energy of the T_1 state of HPhN estimated from the emission spectrum of $Gd(HPhN)_3$ is about 18,300 cm^{-1}. The energies of the singlet and triplet states of dpp, phen and DDXPO are significantly higher than those for the HPhN ligand (e.g., E_{S1} = 27,930 cm^{-1}, E_{T1} = 21,830 cm^{-1} for phen;[72] E_{S1} = 31,850 cm^{-1}, E_{T1} = 23,470 cm^{-1} for DDXPO, **Figure 3**).[61] Thus, these ligands are very likely not to be involved in the sensitization process if the excitation with

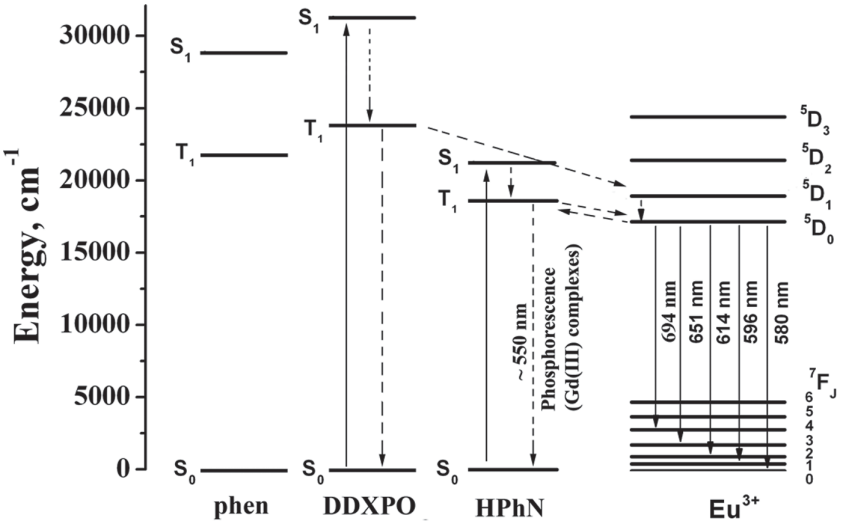

Figure 3. Jablonski diagram for the energy levels of Eu(III) and the respective ligands. The energy levels for the *dpp* ligand are similar to those of *phen* and omitted for simplicity.

visible light is performed. The energy of the S_1 state of the free HPhN ligand estimated from the fluorescence spectrum at 77K is about 22,600 cm^{-1} and about 21,500 cm^{-1} in coordinated state as calculated from the difference in position of the absorption bands of the coordinated and free ligand. Thus, the energy gap between S_1 and T_1 levels of the HPhN is only 3,200 cm^{-1} which is significantly smaller than for known visible light-excitable Eu(III) complexes showing bright luminescence (e.g., 4,200 cm^{-1} for a dipyrazolyltriazine-based ligand[52] and 5,000 cm^{-1} for a pi-extended acridone derivative).[51] Thus, HPhN represents a rather unique antenna chromophore which can be efficiently excited above 460 nm and yet enables efficient sensitization of Eu(III) luminescence.

Since the T_1 level of HPhN in the complexes is located below the $^5D_1$ level of Eu^{3+} (E = 19,000 cm^{-1}) only population of the $^5D_0$ level (E = 17,500 cm^{-1}) appears to be possible (Figure 3). The energy gap between the T_1 level of HPhN and the $^5D_0$ level of Eu^{3+} is very small (500-800 cm^{-1}). This is expected to favor thermally activated back energy transfer and reduce the efficiency of sensitization. Nevertheless, the sensitization is surprisingly efficient even at room temperature (albeit in rather rigid polymer matrix) since the quantum yields of Eu^{3+} luminescence are about 20% (Table 1). A possible explanation for this phenomenon is high rigidity of the HPhN ligand (compared e.g., to β-diketones) which dramatically reduces nonradiative deactivation of the excited triplet state. Indeed, the related work demonstrates that the BF_2-chelated HPhN possesses extraordinary long phosphorescence decay time of about 300 ms.[73] Thus, back energy transfer is unlikely to significantly reduce the luminescence quantum yields and the main deactivation passway is the emission from $^5D_0$ level of Eu(III). However, the back energy transfer may be responsible for extraordinary efficient quenching by molecular oxygen which will be discussed below.

Oxygen-Sensing Properties of the Eu(III) Complexes: The luminescence of virtually all known Eu(III) complexes is barely affected by molecular oxygen, which is due to rather weak interaction of the partly filled f-orbitals (shielded by the 4d and 5p electrons) with the environment and quenchers. In fact, optical oxygen sensors based on the lanthanide complexes show poor sensitivity and quenching even at 100% O_2 does not exceed factor of 4.[43–48] As will be shown below, the proximity of the T_1 level of HPhN and the $^5D_0$ level of Eu^{3+} significantly improves the oxygen-sensing capabilities due to back energy transfer from the Eu^{3+} to the HPhN ligand. In fact, the quenching of the T_1 state of the organic and metal-organic compounds by molecular oxygen is typically very efficient and is limited only by diffusion of the interacting species. Because the levels $^5D_0$ of the Eu(III) and T_1 of the ligand are nearly resonant (Figure 3), both forward and back energy-transfer processes occur resulting in a thermodynamic equilibrium between these two states. Therefore, the oxygen quenching of the long-living ligand triplet states gives rise to a corresponding strong decrease of the Eu(III) emission intensity and decay time.

Planar optodes were prepared by incorporating the Eu(III) complexes in polystyrene. Many other polymers can also be used; however polystyrene represents one of the most common materials and is popular for it high chemical stability, good mechanical properties, adequate oxygen permeability and compatibility with most indicators. Therefore, polystyrene was the matrix of choice in this work. The absorption spectra of the complexes in polystyrene are virtually identical to those in solution (Table 1). In contrast to the solutions of the dyes the sensors are brightly luminescent at room temperature in the absence of oxygen (**Figure 4**, insert). The luminescence spectrum corresponds to the emission of Eu(III) from $^5D_0$ state (Figure S12). The luminescence quantum yields for all the complexes in polystyrene approach 20% (Table 1) which is extraordinary high considering very long excitation wavelengths. Indeed, the quantum yields are comparable to those of typical oxygen indicators, e.g., ruthenium(II)-tris-4,7-diphenyl-1,10-phenanthroline (= Ru-dpp, Φ = 0.37),[74] platinum 5,10,15,20-tetrakis-(2,3,4,5,6-pentafluorphenyl)-porphyrin (= PtTFPP, Φ = 0.09),[75] platinum octaethylporphyrin (Φ = 0.41)[76] and platinum(II) octaethylporphyrin ketone (Φ = 0.12).[12]

The quenching by oxygen is indeed very efficient (Figure 4). Similarly to most state-of-the-art oxygen sensors the Stern-Volmer plots are non-linear. The non-linearity is higher for the decay time plots compared to the intensity plots (Figure 4B and 4C) which is a typical case for the state-of-the-art oxygen sensors. The Stern-Volmer plots can be fitted by so-called "two-site model" assuming localization of the dye in two different environments:[77]

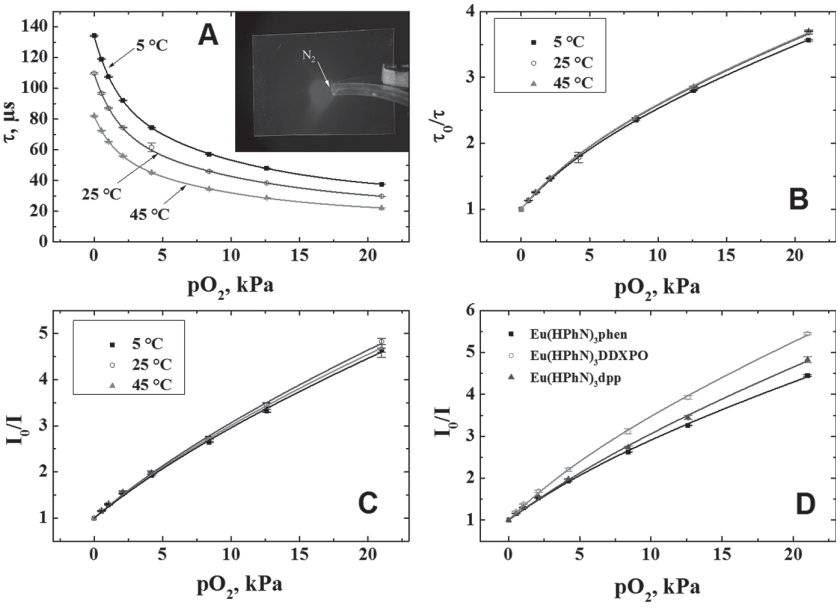

Figure 4. A-C: Calibration plots for Eu(HPhN)$_3$dpp in polystyrene (excitation 465 nm LED); A – lifetime plot, B and C – Stern-Volmer plots for the luminescence decay time and intensity, respectively. D: comparison of the Stern-Volmer plots for the sensors based on the Eu(III) complexes in polystyrene at 25 °C. Insert: photographic image of the planar optode under excitation with 365 nm line of a UV lamp.

$$\frac{I}{I_0}=\frac{\tau}{\tau_0}=\frac{f_1}{1+K_{SV}^1[O_2]}+\frac{f_2}{1+K_{SV}^2[O_2]} \quad (1)$$

where f_1 and f_2 are the fractions of the total emission for each environment, respectively (with $f_1 + f_2$ being 1), and K_{SV}^1 and K_{SV}^2 are the Stern-Volmer constants for each component. Although the equation is physically meaningful for the intensity only, it can often be used to fit the decay time plots as well. The Stern-Volmer plots are very similar for the temperature range from 5 to 45 °C. This behavior may appear rather unusual but is easily explained by rather high dependency of the luminescence decay time τ_0 on temperature (Figure 4A). For example, in case of Eu(HPhN)$_3$dpp/PS sensor the decay times decrease from 134.2 µs at 5 °C to 81.6 µs at 45 °C. Thus, despite very similar K_{SV}^1 values (0.29, 0.30 and 0.30 kPa^{-1} for 5, 25 and 45 °C, respectively; Table S3) the bimolecular quenching constants $k_q = K_{SV}/\tau_0$ are significantly different and increase with temperature (2.1, 2.7 and 3.7 Pa$^{-1}\cdot$s^{-1}, respectively).

The sensitivity of the sensors can be tuned by choosing the Eu(III) complex (Figure 4D). The Stern-Volmer constant is the lowest for Eu(HPhN)$_3$phen (0.27 kPa^{-1} at 25 °C, Table S3) and the highest for Eu(HPhN)$_3$DDXPO (0.53 kPa^{-1}) and Eu(HPhN)$_3$dpp occupies intermediate position. This correlates well with the luminescence decay times in the absence of oxygen (Table 1) which are 93, 110 and 128 µs for Eu(HPhN)$_3$phen, Eu(HPhN)$_3$dpp and Eu(HPhN)$_3$DDXPO, respectively. The k_q values for the sensors based on the new Eu(III) complexes (Table S3) are very similar to those of the common oxygen sensors based on PtTFPP (k_q = 3.5 Pa^{-1}s^{-1})[78] or Ru-dpp in the same polymer (k_q = 2.89 Pa^{-1}s^{-1}).[78] For comparison, the k_q values for the state-of-the-art sensors based on Eu(III) complexes are much lower (e.g., k_q ~ 0.04 Pa^{-1}s^{-1}[79] or 0.1 Pa^{-1}s^{-1}).[45]

Figure 5 compares the emission spectra of the sensors based on the new Eu(III) chelates with those of the state-of-the-art oxygen sensors. The complexes of iridium(III) bis(benzothiazol-2-yl)-7-(diethylamino)-coumarin)(acetylacetonate) (= Ir(C$_S$)$_2$acac), Ru-dpp and PtTFPP emit in yellow-red part of the spectrum. The emission of the indicators is rather broad: FWHM is 32, 25 and 90 nm for Ir(C$_S$)$_2$acac, PtTFPP and Ru-dpp respectively. The second less intense band in case of Ir(C$_S$)$_2$acac and PtTFPP should also be considered. On the contrary, about 80% of the total luminescence of the Eu(III) complexes originates from the $^5D_0 \rightarrow {}^7F_2$ transition (FWHM ~ 4 nm). This very narrow emission is particularly valuable design of multiplexing assays and multi-parameter sensors. Evidently, when using the new Eu(III) complexes virtually the whole spectral region is available for other indicators or labels. Also, the new sensors can be used for measurements at bright daylight. No optical isolation is necessary since the emission of the indicator can be isolated with very narrow interference filters. In the case of conventional indicators the photodetector can be saturated in these conditions.

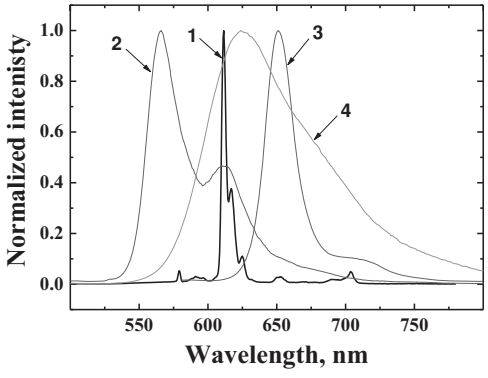

Figure 5. Emission spectrum of Eu(HPhN)$_3$ dpp in polystyrene (1) compared to the emission spectra of Ir(C$_S$)$_2$acac (2), PtTFPP (3) and Ru-dpp (4) in the same polymer.

Oxygen-Sensing Properties of the Gd(III) Complexes: Similarly to efficient emission in frozen organic solvents at 77K, bright phosphorescence is also observed in anoxic conditions at room temperature for the dyes embedded in polymers such as polystyrene (**Figure 6**A(insert), Figure S13). The emission bands are almost identical for Gd(HPhN)$_3$phen and Gd(HPhN)$_3$dpp, but a small bathochromic shift is observed in case of Gd(HPhN)$_3$DDXPO. The emission quantum yields in polystyrene are about 50% (Table 1) which is a very high value for phosphorescent metal complexes. Such intense emission is even more impressive considering that the phosphorescence decay times are rather long (1.3-2 ms, Table 1). To the best of our knowledge there are no phosphorescent metal complexes combining such long decay times and high emission efficiency. Thus, the Gd(III) complexes represent a new class of phosphorescent emitters which combine visible light excitation, very strong emission and long decay times and do not rely on rather expensive platinum group metals such as commonly used platinum, palladium, iridium and ruthenium.

As expected from the long phosphorescence decay times of the Gd(III) complexes, the emission of the polystyrene-based materials is completely quenched in air (Figure 6). The quenching efficiency is about 20-fold higher than for the Eu(III) complexes. Notably, the bimolecular quenching constants k_q are similar for both complex types (Table S3 and S4). In contrast to the Eu(III) complexes, the temperature dependency of the τ_0 is rather low (0.07–0.25%/K, Table S3). Again, the Stern-Volmer plots show better linearity for the luminescence intensity compared to the decay time measurements (Figure 6B and 6C). In full analogy to the Eu(III) complexes fine tuning of the oxygen sensitivity is possible by choosing the appropriate complex (Figure 6D). It should be noted that polystyrene represents only a model matrix chosen for easy comparison with the existing sensors. Polymers with significantly higher oxygen permeability such as ethylcellulose or organically modified silica can be employed to obtain even more sensitive sensors. Thus, the Gd(III) complexes are particularly suitable for designing highly sensitive trace oxygen sensors[80–82] which attract increasing attention in various areas of science and technology, for example for protection of corrosion,[83] tumour hypoxia imaging[84] or investigation of oxygen minimum zones in oceans.[85,86] Paramagnetic character of the Gd(III) complexes can pave the way to some new applications such as simultaneous oxygen sensing and magnetic resonance imaging. Of course, light absorption and scattering in tissues should be considered and synthesis of NIR-emitting probes is likely to be necessary for application in practice.

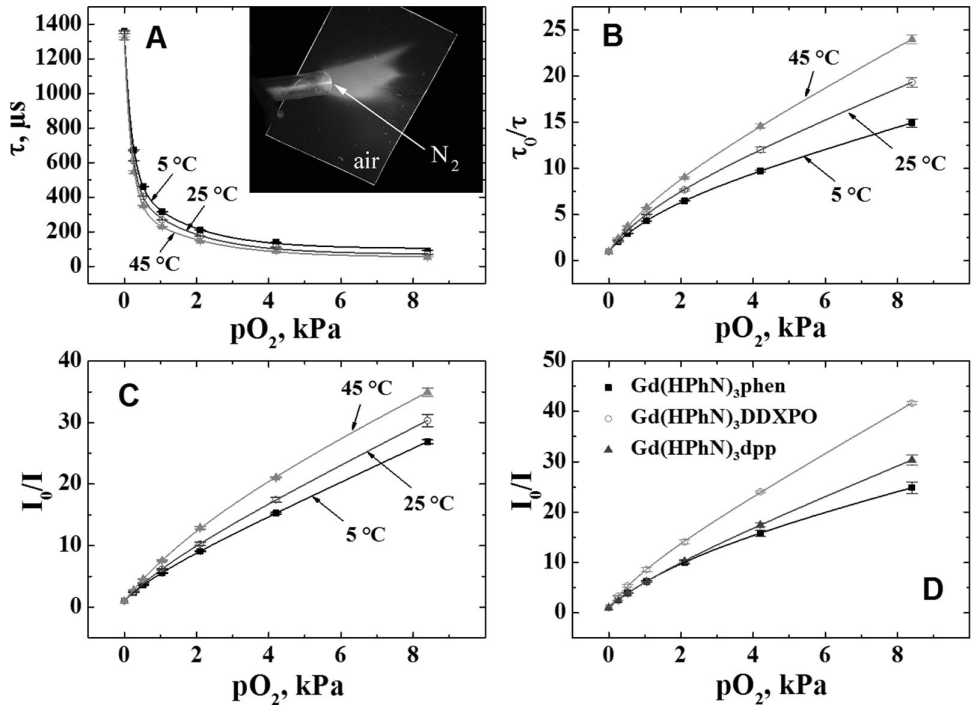

Figure 6. A-C: Calibration plots for $Gd(HPhN)_3dpp$ in polystyrene (excitation 465 nm LED); A – lifetime plot, B and C – Stern-Volmer plots for the luminescence decay time and intensity, respectively. D: comparison of the Stern-Volmer plots for the sensors based on the Gd(III) complexes in polystyrene at 25 °C. Insert: photographic image of the planar optode under excitation with 365 nm line of a UV lamp.

Photostability of the Sensors: Photostability of the sensors in air-saturated conditions was investigated by irradiating the planar optodes with intense blue light (λ_{max} ~ 465 nm, photon flux ~ 4000 μmol·s^{-1}m^{-2}) and monitoring the absorption of the dye. In case of all sensors the absorption gradually decreases with time (**Figure 7**a) and no products absorbing in the visible part of the spectrum are formed. The photodegradation rates are similar for all the Eu(III) complexes, photodegradation being the fastest for $Eu(HPhN)_3DDXPO$ (Figure 7b). The photobleaching is only slightly faster than for the highly photostable Ru-dpp/PS sensors. In fact, only 13–17 % of the dyes are bleached after 2 h of continuous irradiation. It should be noted that the luminescence of Ru-dpp in PS is only minor quenched at air equilibrated conditions (τ_0/τ ~ 1.3). Since oxidation by photosensitized singlet oxygen can be a predominant bleaching mechanism very slow bleaching of Ru-dpp in PS can be explained by low production of singlet oxygen. For comparison, 15% of $Ir(C_S)_2acac$, which is also excitable with blue light, is bleached after 2 min of irradiation.

The photodegradation of the Gd(III) complexes bearing phen and dpp ligands is about 2-folds faster than for the corresponding Eu(III)-complexes (Figure S14). $Gd(HPhN)_3DDXPO$ appears to be significantly less photostable than the Eu(III) and Gd(III) complexes but still much more photostable than $Ir(C_S)_2acac$. Thus, it can be concluded here that the new sensors possess good photostability which is an attractive feature for prolong measurements or measurements at high intensity (e.g., microscopy).

Ratiometric Materials for Imaging Applications: Imaging of oxygen distribution on surfaces is one of the very important applications of oxygen sensors.[87] It is an established method in (marine)biology (e.g., for imaging of oxygen distribution in sediments, biofilms, microbial mats etc.)[88] and becomes

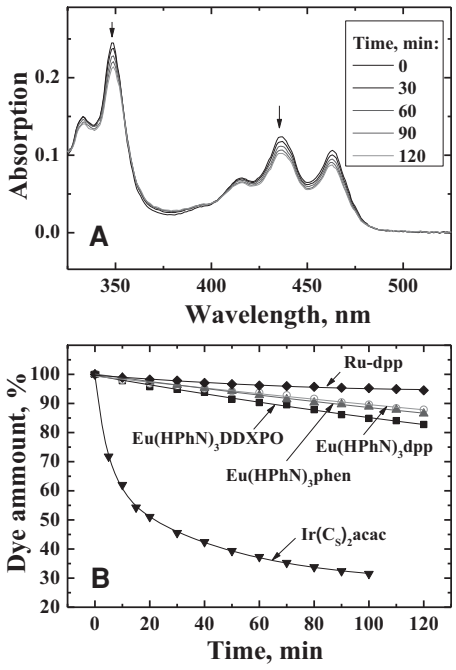

Figure 7. A: absorption spectra of $Eu(HPhN)_3DDXPO$/polystyrene during irradiation with a 465 nm high power LED array (photon flux ~ 4000 μmol·s^{-1}m^{-2}) under air equilibrated conditions; B: photodegradation profiles for the polystyrene sensors based on different oxygen indicators under the same conditions.

increasingly important in other fields of science and technology. Imaging of wound oxygenation on skin[89,90] and imaging of total pressure via pO_2 (pressure-sensitive paints)[91] can be mentioned. Recently, RGB imaging with digital cameras became popular[92–95] most probably due to rather low cost and great availability of the required equipment (such as consumer digital cameras). Although some oxygen sensors for RGB imaging have been proposed it is often challenging to find a pair of dyes (oxygen indicator and a reference dye) which nicely match the color channels of the camera. **Figure 8**A shows that the emission of the Eu(III) complexes in polystyrene almost ideally matches the spectral sensitivity of the red channel of a digital camera. In order to obtain a system for ratiometric read-out polystyrene was co-doped with a fluorescent coumarin dye (C 545T). This lipophilic dye is excitable with blue light and emits in the green part of the spectrum. The luminescence intensity in the green channel is not affected by pO_2; the intensity in the red channel decreases with increasing pO_2 (Figure 8B). These changes correlate well to the emission spectra of the ratiometric sensor (Figure 8A). A non-linear Stern-Volmer plot is observed (Figure 8C). As can be seen from Figure 8D this simple ratiometric sensor allows imaging of oxygen distribution with digital cameras.

Oxygen-Sensitive Nanoparticles: Microscopic imaging of oxygen distribution is a promising method for analysis of enzymatic activity, respiration of mammalian and microbial cells, monitoring of oxygenation in cell cultures and tissues and in the area of food and microbial safety to mention only some of the important applications.[96] The new Eu(III) complexes are attractive for microscopic imaging due to their very narrow emission (which leaves virtually the whole spectral region available for labels or other cellular probes) and excellent photostability (since high light intensities are typically used). Dye-doped nanoparticles are particularly suitable due to their low toxicity, protection of the indicator from undesired interferences (quenchers) by the polymeric shell and the possibility of modification of the nanoparticles surface which enables e.g., cell penetration.[97] Nanosensors can be prepared by several methods, including copolymerization with the monomers, swelling or nanoprecipitation. The $Eu(HPhN)_3dpp$ complex

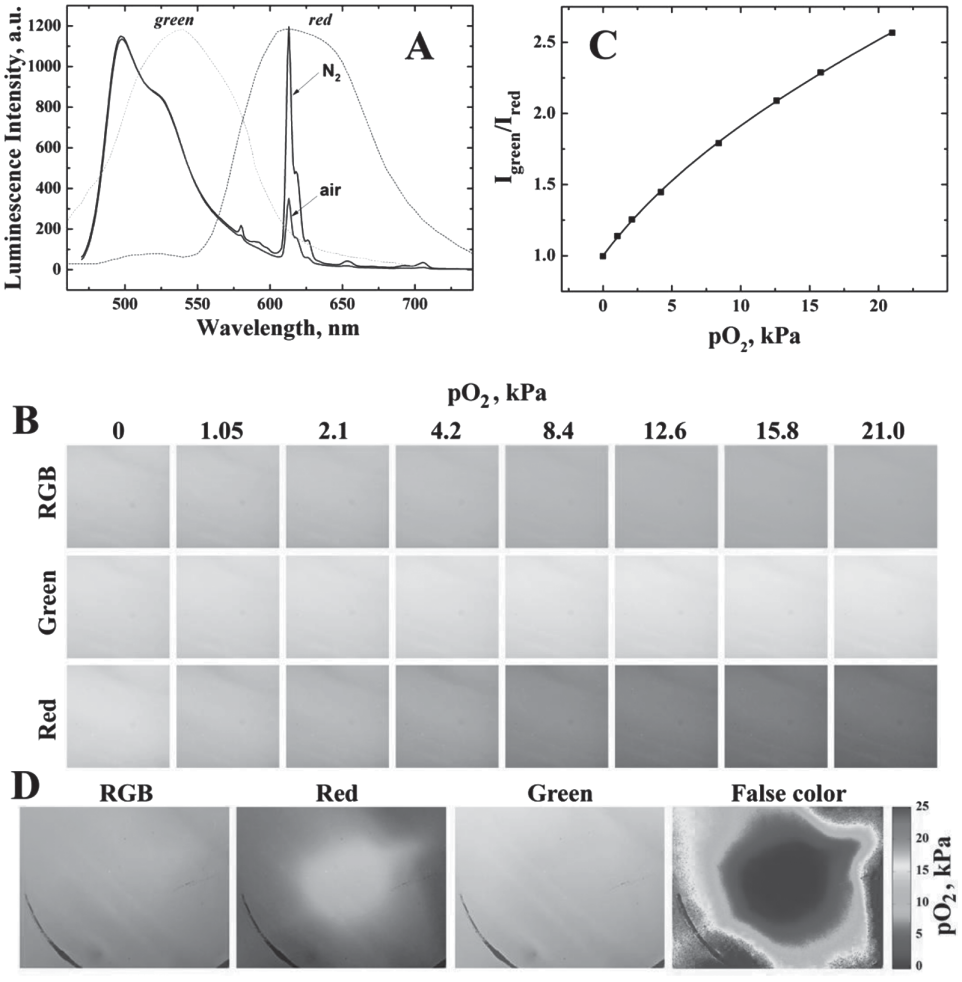

Figure 8. A: Emission spectra of the ratiometric sensor based on coumarin C545T and $Eu(HPhN)_3dpp$ in PS (λ_{exc} 460 nm) and the relative spectral sensitivity for the green and red channels of the digital camera (dashed lines); B: photographic RGB images obtained with a CMOS camera and the images for the red and green channels (λ_{exc} 365 nm); C: Stern-Volmer plot for the luminescence intensity ratio obtained from the photographic images; D: the photographic image of the sensing foil in air with nitrogen stream in the middle of the foil and the respective false-color image of the pO_2 distribution.

was successfully incorporated in two types of oxygen-permeable nanoparticles, namely neutral poly(styrene-block-vinylpyrrolidone) (PS-PVP)[98] and Rl-100, which is a poly(methyl methacrylate) derivative bearing positively charged quaternary ammonium groups.[99] These materials were demonstrated to be suitable for extracellular[98] and intracellular measurements,[99] respectively. In good agreement with the previous work involving other oxygen indicators the size of the PS-PVP beads is significantly larger than that of the Rl-100 beads (Z_{av} = 184 nm, PDI = 0.062 and Z_{av} = 33 nm, PDI = 0.14 for PS-PVP and Rl-100 particles, respectively). The particles show bright luminescence under excitation with the blue light; the luminescence is quenched by molecular oxygen (**Figure 9**a). Excitation spectra (Figure 9b) indicate that the red emission originates from the Eu(III) complex. The sensitivity of both materials is similar (Figure 9c). The other Eu(III) complexes can be also incorporated to fine-tune the sensitivity if necessary. It should be mentioned that a careful consideration of the solvents is required particularly when using the nanoprecipitation procedure (from dilute dye solutions) and polar coordinating solvents (e.g., dimethylformamide) should be avoided to prevent dissociation of the complexes.

The Eu(III) complexes are often used as inert luminescent labels, also in the form of the nanoparticles.[22] Visible-light excitable labels are advantageous because of less interference for the biological systems and broad availability and lower cost of the light sources. A good label should be inert to common interferences including oxygen. Thus, in order to demonstrate the possibility of such applications we incorporated $Eu(HPhN)_3dpp$ in gas-blocking polymethacrylonitrile (PMAN) nanoparticles via precipitation method.[63] The nanoparticles are virtually insensitive to oxygen (Figure 9c). Optimization regarding the size of the nanobeads which are likely to be too large for practical applications (Z_{av} = 180 nm, PDI = 0.126) and availability of the functional groups on their surface is necessary but it is beyond the scope of this work. Incorporation of the Gd(III) complexes inside the nanoparticles is of course also possible. Such materials can be used e.g., for imaging at nearly anoxic conditions.

4. Conclusions

A new class of visible light-excitable Eu(III) and Gd(III) complexes is presented. The unique 8-hydroxyphenalenone antenna ligand featuring a very small singlet-triplet energy gap enables efficient excitation in the blue part of the electromagnetic spectrum. The Eu(III) complexes show rather strong luminescence originating from the Eu(III) ion which is unprecedented for such low energetic excitation. The Gd(III) complexes show very strong room-temperature phosphorescence in polymers in the absence of oxygen with quantum yields of about 50% which places them among the strongest phosphorescent emitters known. In contrast to the state-of-the-art Eu(III) complexes, which luminescence is only minor affected by molecular oxygen, the new dyes show the sensitivity comparable to that

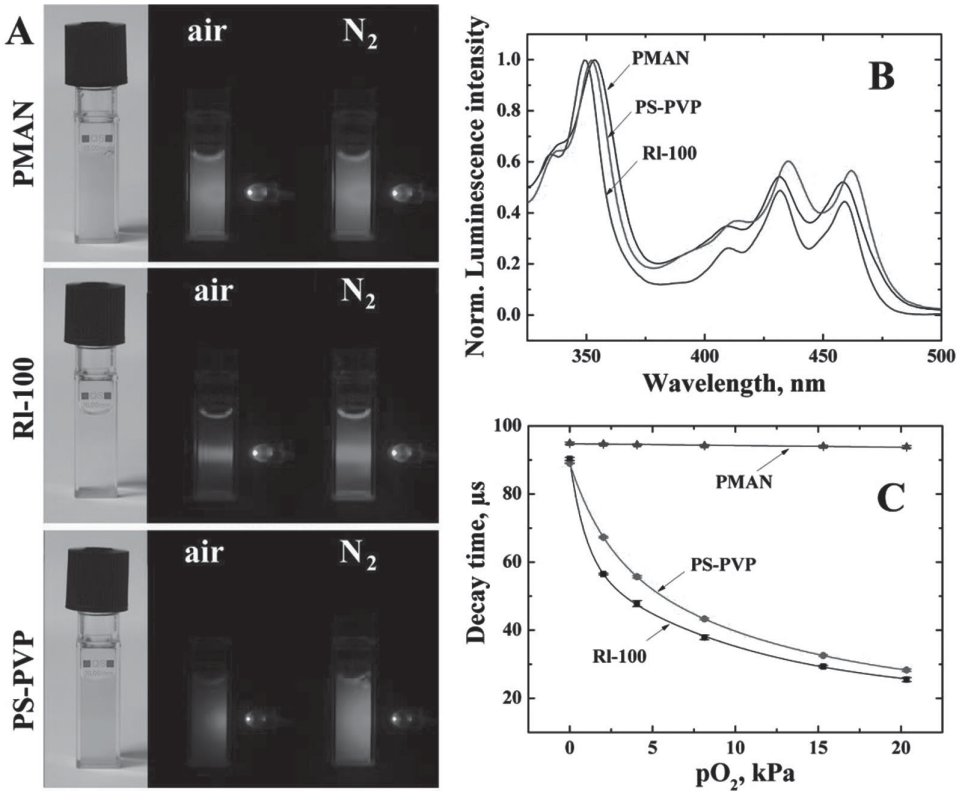

Figure 9. A: photographic images of the aqueous dispersion of the beads (stained with $Eu(HPhN)_3dpp$) under ambient light illumination and in darkness upon excitation with a 465 nm LED; B: excitation spectra of the dispersions of the beads (λ_{em} = 614 nm); C: oxygen sensitivity of the dye-doped nanoparticles.

of the conventional oxygen sensing materials. The very narrow emission of the indicators makes them suitable for application in multi-parameter sensors and in microscopy. The nanoparticles based on the new complexes can be particularly promising for microscopic extra- and intracellular imaging where narrow emission and high photostability are especially valuable. RGB imaging of oxygen distribution with consumer cameras can also be realized due to excellent compatibility of the Eu(III) emission with the sensitivity of the red channel of a digital camera. The Gd(III) complexes feature very long phosphorescence decay times exceeding 1ms and very high sensitivity even in polymers of moderate oxygen permeability such as polystyrene. This makes them particularly attractive for preparation of trace oxygen sensors. Last but not least, the new indicators can be prepared in only two steps from cheap starting materials which do not include expensive platinum group metals. Thus the dyes can pave the way to the applications where low cost of the indicator is essential (e.g., food packaging). Additionally, due to their paramagnetic character, the Gd(III) complexes may be promising for simultaneous oxygen sensing and magnetic resonance imaging. They may also be a platform for designing low cost triplet emitters in OLED applications.

Supporting Information

Supporting Information is available from the Wiley Online Library or from the author.

Acknowledgements

The financial support from the European Research Council (Project "Oxygen", N 267233) is gratefully acknowledged.

Received: May 30, 2014
Revised: July 3, 2014
Published online: August 22, 2014

[1] Y. Amao, *Microchim. Acta* **2003**, *143*, 1.
[2] O. S. Wolfbeis, *J. Mater. Chem.* **2005**, *15*, 2657.
[3] M. Quaranta, S. M. Borisov, I. Klimant, *Bioanal. Rev.* **2012**, *4*, 115.
[4] X. Wang, O. S. Wolfbeis, *Chem. Soc. Rev.* **2014**, *43*, 3666.
[5] H. J. Kim, Y. C. Jeong, J. I. Rhee, *Talanta* **2008**, *76*, 1070.
[6] H. Lam, G. Rao, J. Loureiro, L. Tolosa, *Talanta* **2011**, *84*, 65.
[7] D. García-Fresnadillo, M. D. Marazuela, M. C. Moreno-Bondi, G. Orellana, *Langmuir* **1999**, *15*, 6451.
[8] Y. Amao, T. Miyashita, I. Okura, *J. Fluorine Chem.* **2001**, *107*, 101.
[9] S. A. Vinogradov, D. F. Wilson, *J. Chem. Soc., Perkin Trans. 2* **1995**, 103.
[10] O. S. Finikova, A. Y. Lebedev, A. Aprelev, T. Troxler, F. Gao, C. Garnacho, S. Muro, R. M. Hochstrasser, S. A. Vinogradov, *Chem Phys Chem* **2008**, *9*, 1673.
[11] S. M. Borisov, G. Nuss, I. Klimant, *Anal. Chem.* **2008**, *80*, 9435.
[12] D. B. Papkovsky, G. V. Ponomarev, W. Trettnak, P. O'Leary, *Anal. Chem.* **1995**, *67*, 4112.
[13] G. Khalil, M. Gouterman, S. Ching, C. Costin, L. Coyle, S. Gouin, E. Green, M. Sadilek, R. Wan, J. Yearyean, B. Zelelow, *J. Porphyr. Phthalocya.* **2002**, *6*, 135.
[14] S. M. Borisov, G. Zenkl, I. Klimant, *ACS Appl. Mater. Interfaces* **2010**, *2*, 366.
[15] M. C. DeRosa, D. J. Hodgson, G. D. Enright, B. Dawson, C. E. B. Evans, R. J. Crutchley, *J. Amer. Chem. Soc.* **2004**, *126*, 7619.
[16] M. C. DeRosa, P. J. Mosher, G. P. A. Yap, K.-S. Focsaneanu, R. J. Crutchley, C. E. B. Evans, *Inorg. Chem.* **2003**, *42*, 4864.
[17] C. S. K. Mak, D. Pentlehner, M. Stich, O. S. Wolfbeis, W. K. Chan, H. Yersin, *Chem. Mater.* **2009**, *21*, 2173.
[18] W. Xu, K. A. Kneas, J. N. Demas, B. A. DeGraff, *Anal. Chem.* **1996**, *68*, 2605.
[19] K. A. Kneas, W. Xu, J. N. Demas, B. A. DeGraff, A. P. Zipp, *J. Fluoresc.* **1998**, *8*, 295.
[20] C. S. Smith, K. R. Mann, *J. Amer. Chem. Soc.* **2012**, *134*, 8786.
[21] C. S. Smith, C. W. Branham, B. J. Marquardt, K. R. Mann, *J. Amer. Chem. Soc.* **2010**, *132*, 14079.
[22] J.-C. G. Bünzli, *Chem. Rev.* **2010**, *110*, 2729.
[23] I. Hemmila, V. Laitala, *J. Fluoresc.* **2005**, *15*, 529.
[24] E. J. New, D. Parker, D. G. Smith, J. W. Walton, *Curr. Opin. Chem. Biol.* **2010**, *14*, 238.
[25] J.-C. G. Bünzli, C. Piguet, *Chem. Soc. Rev.* **2005**, *34*, 1048.
[26] D. Parker, *Coord. Chem. Rev.* **2000**, *205*, 109.
[27] M. Mitsuishi, S. Kikuchi, T. Miyashita, Y. Amao, *J. Mater. Chem.* **2003**, *13*, 2875.
[28] B. Zelelow, G. E. Khalil, G. Phelan, B. Carlson, M. Gouterman, J. B. Callis, L. R. Dalton, *Sensor. Actuat. B-Chem.* **2003**, *96*, 304.
[29] M. I. J. Stich, S. Nagl, O. S. Wolfbeis, U. Henne, M. Schaeferling, *Adv. Funct. Mater.* **2008**, *18*, 1399.
[30] S. Borisov, I. Klimant, *J. Fluoresc.* **2008**, *18*, 581.
[31] H. Peng, M. I. J. Stich, J. Yu, L. Sun, L. H. Fischer, O. S. Wolfbeis, *Adv. Mater.* **2010**, *22*, 716.
[32] R. Pal, D. Parker, *Chem. Commun.* **2007**, 474.
[33] A. Lobnik, N. Majcen, K. Niederreiter, G. Uray, *Sensor. Actuat. B-Chem.* **2001**, *74*, 200.
[34] R. Pal, D. Parker, *Org. Biomol. Chem.* **2008**, *6*, 1020.
[35] J. Hynes, T. C. O'Riordan, A. V. Zhdanov, G. Uray, Y. Will, D. B. Papkovsky, *Anal. Biochem.* **2009**, *390*, 21.
[36] J. D. Moore, R. L. Lord, G. A. Cisneros, M. J. Allen, *J. Am. Chem. Soc.* **2012**, *134*, 17372
[37] Y. Bretonniere, M. J. Cann, D. Parker, R. Slater, *Org. Biomol. Chem.* **2004**, *2*, 1624.
[38] D. G. Smith, R. Pal, D. Parker, *Chem. – Eur. J.* **2012**, *18*, 11604.
[39] D. Parker, J. Yu, *Chem. Commun.* **2005**, 3141.
[40] R. Pal, D. Parker, L. C. Costello, *Org. Biomol. Chem.* **2009**, *7*, 1525.
[41] O. S. Wolfbeis, A. Dürkop, M. Wu, Z. Lin, *Angew. Chem. Int. Ed.* **2002**, *41*, 4495.
[42] Y. Chen, W. Guo, Z. Ye, G. Wang, J. Yuan, *Chem. Commun.* **2011**, *47*, 6266.
[43] Y. Amao, I. Okura, T. Miyashita, *B. Chem. Soc. JPN.* **2000**, *73*, 2663.
[44] Y. Amao, I. Okura, T. Miyashita, *Chem. Lett.* **2000**, 934.
[45] Y. Wang, B. Li, L. Zhang, Q. Zuo, P. Li, J. Zhang, Z. Su, *Chem Phys Chem* **2011**, *12*, 349.
[46] Q. Zuo, B. Li, L. Zhang, Y. Wang, Y. Liu, J. Zhang, Y. Chen, L. Guo, *J. Solid State Chem.* **2010**, *183*, 1715.
[47] L. Songzhu, D. Xiangting, W. Jinxian, L. Guixia, Y. Wenshen, J. Ruokun, *Spectrochim. Acta A* **2010**, *77*, 885.
[48] N. Feng, J. Xie, D. Zhang, *Spectrochim. Acta A* **2010**, *77*, 292.
[49] A. Dadabhoy, S. Faulkner, P. G. Sammes, *J. Chem. Soc., Perkin Trans. 2* **2000**, 2359.
[50] M. H. V. Werts, M. A. Duin, J. W. Hofstraat, J. W. Verhoeven, *Chem. Commun.* **1999**, 799.
[51] E. Deiters, F. Gumy, J.-C. G. Bünzli, *Eur. J. Inorg. Chem.* **2010**, *2010*, 2723.
[52] C. Yang, L.-M. Fu, Y. Wang, J.-P. Zhang, W.-T. Wong, X.-C. Ai, Y.-F. Qiao, B.-S. Zou, L.-L. Gui, *Angew. Chem. Int. Ed.* **2004**, *43*, 5010.
[53] A. Strasser, A. Vogler, *Inorg. Chim. Acta* **2004**, *357*, 2345.
[54] S. M. Borisov, I. Klimant, *Anal. Bioanal. Chem.* **2012**, *404*, 2797.

[55] X. Zhang, T. Xie, M. Cui, L. Yang, X. Sun, J. Jiang, G. Zhang, *ACS Appl. Mater. Interfaces* **2014**, *6*, 2279.
[56] K. N. Raymond, V. C. Pierre, *Bioconj. Chem.* **2005**, *16*, 3.
[57] W. C. Floyd, P. J. Klemm, D. E. Smiles, A. C. Kohlgruber, V. C. Pierre, J. L. Mynar, J. M. J. Fréchet, K. N. Raymond, *J. Amer. Chem. Soc.* **2011**, *133*, 2390.
[58] W.-S. Li, J. Luo, F. Jiang, Z.-N. Chen, *Dalton Trans.* **2012**, *41*, 9405.
[59] R. V. Deun, P. Nockemann, P. Fias, K. V. Hecke, L. V. Meervelt, K. Binnemans, *Chem. Commun.* **2005**, 590.
[60] R. C. Haddon, R. Rayford, A. M. Hirani, *J. Org.Chem.* **1981**, *46*, 4587.
[61] D. B. A. Raj, S. Biju, M. L. P. Reddy, *Dalton Trans.* **2009**, 7519.
[62] S. M. Borisov, I. Klimant, *Microchim. Acta* **2008**, *164*, 7.
[63] S. M. Borisov, T. Mayr, G. Mistlberger, K. Waich, K. Koren, P. Chojnacki, I. Klimant, *Talanta* **2009**, *79*, 1322–1330.
[64] G. Seybold, G. Wagenblast, *Dyes Pigments* **1989**, *11*, 303.
[65] *SAINT*, Bruker AXS Inc., Madison, WI, **2000**.
[66] G. M. Sheldrick, *SADABS: Program for Performing Absorption Corrections to Single-Crystal X-Ray Diffraction Patterns*, University of Göttingen **2002**.
[67] G. M. Sheldrick, *SHELXTL: Suite of Programs for Crystal Structure Analysis, Incorporating Structure Solution (XS), Least- Squares Refinement (XL), and Graphics (XP)*, University Of Göttingen, Göttingen, Germany **2001**.
[68] C. F. Macrae, I. J. Bruno, J. A. Chisholm, P. R. Edgington, P. McCabe, E. Pidcock, L. Rodriguez-Monge, R. Taylor, J. van de Streek, P. A. Wood, *J. Appl.Crystallogr.* **2008**, *41*, 466.
[69] C.-H. Huang, *Rare Earth Coordination Chemistry: Fundamentals and Applications*, John Wiley & Sons (Asia), Singapore **2010**.
[70] P. Mueller, *Crystal Structure Refinement*, Oxford University Press, Oxford UK, **2006**.
[71] B. G. Wybourne, *Phys. Rev.* **1966**, *148*, 317.
[72] B. Yan, H. Zhang, S. Wang, J. Ni, *J. Photoch. Photobio. A* **1998**, *116*, 209.
[73] P. Lehner, C. Staudinger, S. M. Borisov, I. Klimant, *Nat. Commun.* **2014**, *5*, 4460.
[74] P. C. Alford, M. J. Cook, A. P. Lewis, G. S. G. McAuliffe, V. Skarda, A. J. Thomson, J. L. Glasper, D. J. Robbins, *J. Chem. Soc., Perkin Trans. 2* **1985**, 705.
[75] S.-W. Lai, Y.-J. Hou, C.-M. Che, H.-L. Pang, K.-Y. Wong, C. K. Chang, N. Zhu, *Inorg. Chem.* **2004**, *43*, 3724.
[76] A. K. Bansal, W. Holzer, A. Penzkofer, T. Tsuboi, *Chem. Phys.* **2006**, *330*, 118.
[77] E. R. Carraway, J. N. Demas, B. A. DeGraff, J. R. Bacon, *Anal. Chem.* **1991**, *63*, 337.
[78] S. M. Borisov, I. Klimant, *Anal. Chem.* **2007**, *79*, 7501.
[79] J. Sun, G. Hu, Q. She, Z. Zuo, L. Gou, *Spectrochim. Acta A* **2012**, *91*, 192.
[80] S. Nagl, C. Baleizão, S. M. Borisov, M. Schäferling, M. N. Berberan-Santos, O. S. Wolfbeis, *Angew. Chem. Int. Ed.* **2007**, *46*, 2317.
[81] C. Baleizão, S. Nagl, M. Schäferling, M. N. Berberan-Santos, O. S. Wolfbeis, *Anal. Chem.* **2008**, *80*, 6449.
[82] S. M. Borisov, P. Lehner, I. Klimant, *Anal. Chim. Acta* **2011**, *690*, 108.
[83] K. Tanno, *B. Chem. Soc. JPN.* **1964**, *37*, 804.
[84] G. Zhang, G. M. Palmer, M. W. Dewhirst, C. L. Fraser, *Nat. Mater.* **2009**, *8*, 747.
[85] D. A. Stolper, N. P. Revsbech, D. E. Canfield, *Proc. Natl. Acad. Sci. U. S. A.* **2010**, *107*, 18755.
[86] N. P. Revsbech, L. H. Larsen, J. Gundersen, T. Dalsgaard, O. Ulloa, B. Thamdrup, *Limnol. Oceanogr. Meth.* **2009**, *7*, 371.
[87] M. Schäferling, *Angew. Chem. Int. Ed.* **2012**, *51*, 3532.
[88] M. Kuhl, L. Polerecky, *Aquat. Microb. Ecol.* **2008**, *53*, 99.
[89] S. Schreml, R. J. Meier, O. S. Wolfbeis, T. Maisch, R.-M. Szeimies, M. Landthaler, J. Regensburger, F. Santarelli, I. Klimant, P. Babilas, *Exp. Dermatol.* **2011**, *20*, 550.
[90] R. J. Meier, S. Schreml, X. Wang, M. Landthaler, P. Babilas, O. S. Wolfbeis, *Angew. Chem. Int. Ed.* **2011**, *50*, 10893.
[91] O. S. Wolfbeis, *Adv. Mater.* **2008**, *20*, 3759.
[92] M. Larsen, S. M. Borisov, B. Grunwald, I. Klimant, R. N. Glud, *Limnol.Oceanogr. Meth.* **2011**, *9*, 348.
[93] X. Wang, R. J. Meier, M. Link, O. S. Wolfbeis, *Angew. Chem. Int. Ed.* **2010**, *49*, 4907.
[94] R. J. Meier, L. H. Fischer, O. S. Wolfbeis, M. Schäferling, *Sensor. Actuat. B- Chem.* **2013**, *177*, 500.
[95] B. Ungerböck, V. Charwat, P. Ertl, T. Mayr, *Lab Chip* **2013**, *13*, 1593.
[96] D. B. Papkovsky, R. I. Dmitriev, *Chem. Soc. Rev.* **2013**, *42*, 8700.
[97] J. W. Aylott, *Analyst* **2003**, *128*, 309.
[98] S. M. Borisov, T. Mayr, I. Klimant, *Anal. Chem.* **2008**, *80*, 573.
[99] A. Fercher, S. M. Borisov, A. V. Zhdanov, I. Klimant, D. B. Papkovsky, *ACS Nano* **2011**, *5*, 5499.